

Supporting Information

Achieving 17.5% efficiency of polymer solar cells via donor and acceptor layered optimization strategy

Wenjing Xu,^a Xiong Li,^{b*} Sang Young Jeong,^c Jae Hoon Son,^c Zhengji Zhou,^{d*} Qiuju Jiang,^e Han Young Woo,^c Qinghe Wu,^e Xixiang Zhu,^a Xiaoling Ma,^a Fujun Zhang^{a*}

^a Key Laboratory of Luminescence and Optical Information, Ministry of Education, Beijing Jiaotong University, 100044, Beijing, China.

^b Department of Physics, Beijing Technology and Business University, 100048, Beijing, China.

^c Organic Optoelectronic Materials Laboratory, Department of Chemistry, College of Science, Korea University, 02841, Seoul, Republic of Korea.

^d Key Lab for Special Functional Materials, Ministry of Education, National and Local Joint Engineering Research Center for High-Efficiency Display and Lighting Technology, and School of Materials, Henan University, 475004, Kaifeng, Henan Province, China.

^e Department of Chemistry and Key Laboratory for Preparation and Application of Ordered Structural Materials of Guangdong, Shantou University, 515063, Guangdong, China.

Corresponding author: lixiong@btbu.edu.cn (Xiong), zzj@henu.edu.cn (Zhengji),

fjzhang@bjtu.edu.cn (Fujun)

Experimental section

Device Fabrication:

The patterned indium tin oxide (ITO) coated glass substrates (15 Ω per square) were cleaned via sequential sonication in detergent, de-ionized and ethanol and then blow-dried by high-purity nitrogen. All pre-cleaned ITO substrates were treated by oxygen plasma for 1 minute to improve their work function and clearance. Subsequently, poly(3,4-ethylenedioxythiophene): poly(styrene sulfonate) (PEDOT: PSS, purchased from H.C. Starck co. Ltd.) solution was spin-coated on ITO substrates at 5000 rpm for 40 s and dried at 150 °C for 15 min in atmospheric air. Then ITO substrates coated with PEDOT: PSS films were transferred into a high-purity nitrogen-filled glove

box. Polymer donor PNTB6-Cl was provided by Prof. Qinghe Wu and Y6 was purchased from Solarmer Materials Inc. The blend active layers were spin coated from 16.4 mg/ml chlorobenzene solution (PNTB6-Cl:Y6=1:1.2, without or with 0.5 vol% DPE and DFB) at 3000 rpm for 30 s. The donor layers were spin coated from 7.2 mg/ml PNTB6-Cl chlorobenzene solution (without or with 0.5 vol% DPE) at 2300 rpm for 30 s, then the acceptor layers were spin coated from 9.2 mg/ml Y6 chloroform solution (without or with 0.5 vol% DFB) at 2000 rpm for 30 s on the top of the donor layers. The 18 μ l solution was picked up for each spin-coating fabrication. Then, the donor and acceptor layers were thermally annealed at 110 °C for 5 min. Interfacial layer of PNDIT-F3N was deposited by spin-coating solution in methanol (0.5 mg/ml) at 2000 rpm for 30 s. PNDIT-F3N was dissolved in methanol with the addition of 0.25 vol% acetic acid to prepare a 0.5 mg/ml solution. The PNDIT-F3N solution was spin-coated onto the active layers at 2000 rpm for 40 s. Finally, 100 nm Ag layer was deposited by thermal evaporation through a shadow mask under the vacuum of 5×10^{-4} Pa conditions. The active area is approximately 3.8 mm², defined by the overlapping area of ITO anode and Ag cathode.

Device Measurement

The current-voltage (J - I) curves of all PSCs were measured in a high-purity nitrogen-filled glove box using a Keithley 2400 source meter. AM 1.5G irradiation at 100 mW cm⁻² was provided by An XES-40S2 (SAN-EI Electric Co., Ltd.) solar simulator (AAA grade, 70×70 mm² photobeam size), which was calibrated by standard silicon solar cells (purchased from Zolix INSTRUMENTS CO. LTD). The ultraviolet-visible (UV-Vis) absorption spectra of films were obtained using a Shimadzu UV-3101 PC spectrometer. The external quantum efficiency (EQE) spectra of PSCs were measured in the air conditions by a Zolix Solar Cell Scan 100. Photoluminescence (PL) spectra of films were measured by a HORIBA Fluorolog®-3 spectrofluorometer system. The morphology of the active layers was investigated by AFM using a Dimension Icon AFM (Bruker) in a tapping mode. The samples for AFM characterization were prepared under the same conditions compared with the active layers of the PSCs. Grazing incidence wide angle X-ray scattering (GIWAXS) measurements were accomplished at PLS-II 9A U-SAXS beamline of the Pohang Accelerator Laboratory in Korea. Transient photovoltage (TPV), transient photocurrent (TPC) and photo-charge extraction linear increasing voltage (Photo-CELIV) were conducted with the PaioCarrier measurement system (FLUXiM AG, Switzerland). A high-power white LED is utilized as light source for TPV, TPC and

photo-CELIV measurements. The integrated power of the LED is 72mW cm⁻², and the spectrum distribution is mainly in the wavelength range of 440-470 nm and 540-630 nm, and the peak value located at 460 nm and 550 nm. Schematic diagram of the photo-CELIV and triangular pulse in reverse bias after photo-exciting the sample are as follows:

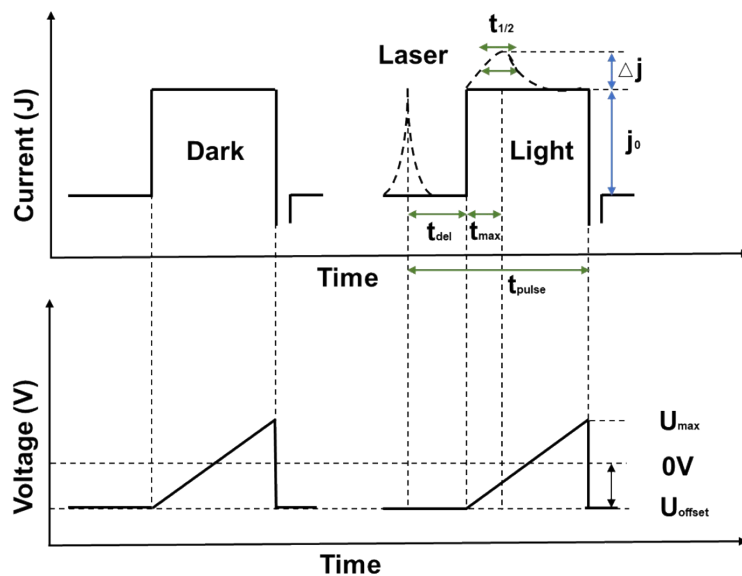


Figure S1. Schematic diagram of the photo-CELIV and triangular pulse in reverse bias after photo-exciting the sample.

The photogenerated exciton distribution in the active layer can be calculated according to the optical field distribution and absorption coefficient of active layer. Exciton generation rate in the active layers can be estimated according to the equation (1)^{1,2}:

$$\rho(\lambda) \propto \frac{|E(\lambda)|^2}{h\nu} \times \alpha(\lambda) \times \eta_D \quad (1)$$

Here, $\rho(\lambda)$ is the exciton generation rate, $|E(\lambda)|^2$ is the optical field intensity, $\alpha(\lambda)$ is the absorption coefficient, and η_D is the exciton dissociation coefficient. The η_D can be considered as constant in the entire active layers. The $|E(\lambda)|^2$ in the active layer of PSCs was calculated using Transfer Matrix method.

Transfer Matrix calculation:^{3,4}

Light is considered as a plane wave in transfer matrix theory. Only the light incident perpendicular to the substrate will be considered for PSCs devices. The optical field at any point in the device is a complex quantity and is given a positive superscript $E^+(x)$ for waves traveling from left to right and a negative superscript $E^-(x)$ for waves traveling from right to left, as shown in **Scheme 1**. The

devices are stacked of m layers, each of which is described by its complex index of refraction $\tilde{n} = n + i\kappa$ and thickness d , sandwiched between the glass substrate and the atmosphere. The behavior of light at the interface between two layers, j and k , can be described by a 2×2 matrix that contains the complex Fresnel coefficients. This matrix \mathbf{I}_{jk} is known as the interface matrix, which for normal incidence can be given as:

$$I_{ij} = \begin{bmatrix} (\tilde{n}_j + \tilde{n}_k)/2\tilde{n}_j & (\tilde{n}_j - \tilde{n}_k)/2\tilde{n}_j \\ (\tilde{n}_j - \tilde{n}_k)/2\tilde{n}_j & (\tilde{n}_j + \tilde{n}_k)/2\tilde{n}_j \end{bmatrix} \quad (2)$$

Similarly, the effect on the optical field from propagating through each layer is described by a 2×2 matrix \mathbf{L}_j known as the layer matrix:

$$L_j = \begin{bmatrix} e^{-i\xi_j d_j} & 0 \\ 0 & e^{i\xi_j d_j} \end{bmatrix} \quad (3)$$

where $\xi_j = 2\pi\tilde{n}_j/\lambda$ and λ is the wavelength of the light. The components of the optical field within the substrate (subscript 0) are related to those in the atmosphere (subscript $m+1$) by the total transfer matrix \mathbf{S} :

$$\begin{bmatrix} E_0^+ \\ E_0^- \end{bmatrix} = \mathbf{S} \begin{bmatrix} E_{m+1}^+ \\ E_{m+1}^- \end{bmatrix} \quad (4)$$

where \mathbf{S} is the product of all interface and layer matrices

$$\mathbf{S} = \begin{bmatrix} S_{11} & S_{12} \\ S_{21} & S_{22} \end{bmatrix} = \left(\prod_{v=1}^m I_{(v-1)v} L_v \right) I_{m(m+1)} \quad (5)$$

The field quantities in equation (4) are those that exist at the boundaries with the stack of m layers that makes up the active part of the device. Considering light incidents from the substrate side only requires that $E_{m+1}^- = 0$, allowing the reflection and transmission coefficients of the multilayer stack to be expressed as

$$r = S_{21}/S_{11} \quad (6a)$$

$$t = 1/S_{11} \quad (6b)$$

To determine the optical field at a distance x within layer j of the device, one must add the left- and right-traveling waves,

$$E_j(x) = E_j^+(x) + E_j^-(x) \quad (7)$$

To find these two latter quantities, equation (5) is split into two partial transfer matrices by the relation $S = S'_j L'_j S''_j$. These two matrices are separately defined as

$$S'_j = \begin{bmatrix} S'_{j11} & S'_{j12} \\ S'_{j21} & S'_{j22} \end{bmatrix} = \left(\prod_{v=1}^{j-1} I_{(v-1)v} L_v \right) I_{m(m+1)} \quad (8a)$$

$$S''_j = \begin{bmatrix} S''_{j11} & S''_{j12} \\ S''_{j21} & S''_{j22} \end{bmatrix} = \left(\prod_{v=j+1}^m I_{(v-1)v} L_v \right) I_{m(m+1)} \quad (8b)$$

Algebraic manipulation then allows equation (7) to be expressed in terms of known quantities,

$$E_j(x) = t_j^+ [e^{i\xi_j x} + r_j'' e^{i\xi_j(2d_j - x)}] E_0^+ \quad (9)$$

where E_0^+ is the optical field inside the substrate incident on layer 1,

$$t_j^+ = [S'_{j11} + S'_{j12} r_j'' e^{2i\xi_j d_j}]^{-1} \quad (10)$$

And

$$r_j^+ = S''_{j21} / S''_{j11} \quad (11)$$

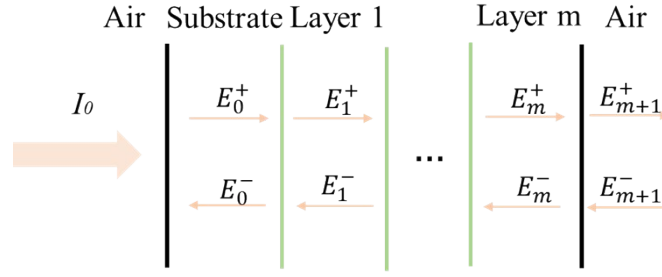
The substrate cannot be included directly in the transfer-matrix calculation due to the large thickness of the glass \sim (1.0 mm). However, to obtain quantitatively accurate results for the intensity in each layer, the effect of the substrate is included by summing the intensities within the glass as opposed to the optical fields. The intensity of light incident on the multilayer from within the substrate I_S is then given by

$$I_S = I_0 \frac{T_S e^{-\alpha_s d_s}}{1 - R R_S e^{-2\alpha_s d_s}} = I_0 T_{int} \quad (12)$$

where I_0 is the light intensity incident on the device, R and T are the reflectance and transmittance of the multilayer stack, and variables subscripted with S represent values for the substrate. This allows us to define an internal transmittance T_{int} for the substrate in terms of the absorption coefficient $\alpha_j = 4\pi\kappa_j/\lambda$. By using equation (9) and equation (12), the light intensity at a distance x within layer j of the device can be expressed as

$$I_j(x) = I_0 T_{int} |t_j^+|^2 \text{Re} \left(\frac{\tilde{n}_j}{\tilde{n}_s} \right) \left\{ e^{-\alpha_j x} + \rho_j''^2 e^{-\alpha_j(2d_j - x)} + 2\rho_j'' e^{-\alpha_j d_j} \cos \frac{4\pi n_j(d_j - x)}{\lambda} + \delta_j'' \right\} \quad (13)$$

Where ρ_j'' is the argument and δ_j'' is the phase of the quantity in equation (11). The optical field intensity at every point in the device can be calculated by equation (13).



Scheme 1. Schematic diagram of incident light transmission in the device consisting of a stack of m layers.

The structure of electron-only devices is ITO/ZnO/active layer/PNDIT-F3N/Al and the structure of hole-only devices is ITO/PEDOT:PSS/active layer/MoO₃/Ag. The fabrication conditions of the active layer films are same with those for the PSCs. The charge mobilities are generally described by the Mott-Gurney equation (14)⁵⁻⁷:

$$J = \frac{9}{8} \varepsilon_r \varepsilon_0 \mu \frac{V^2}{L^3} \quad (14)$$

where J is the current density, ε_0 is the permittivity of free space (8.85×10^{-14} F/cm), ε_r is the dielectric constant of used materials, μ is the charge mobility, V is the applied voltage and L is the active layer thickness. The ε_r parameter is assumed to be 3 as a typical value for organic materials. In organic materials, charge mobility is usually field dependent and can be described by the disorder formalism, typically varying with electric field, $E=V/L$, according to the equation (15):

$$\mu = \mu_0 \exp\left[0.89\gamma \sqrt{\frac{V}{L}}\right] \quad (15)$$

where μ_0 is the charge mobility at zero electric field and γ is a constant. Then, the Mott-Gurney equation can be described by (16)⁸⁻¹⁰:

$$J = \frac{9}{8} \varepsilon_r \varepsilon_0 \mu_0 \frac{V^2}{L^3} \exp\left[0.89\gamma \sqrt{\frac{V}{L}}\right] \quad (16)$$

In this case, the charge mobilities were estimated using the following equation (17):

$$\ln\left(\frac{JL^3}{V^2}\right) = 0.89\gamma \sqrt{\frac{V}{L}} + \ln\left(\frac{9}{8} \varepsilon_r \varepsilon_0 \mu_0\right) \quad (17)$$

Additional experimental results

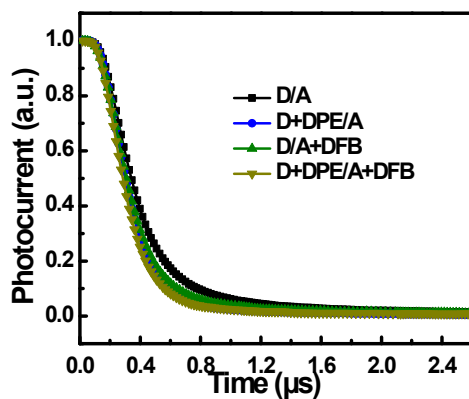


Figure S2. Transient photocurrent curves of all LbL-PSCs.

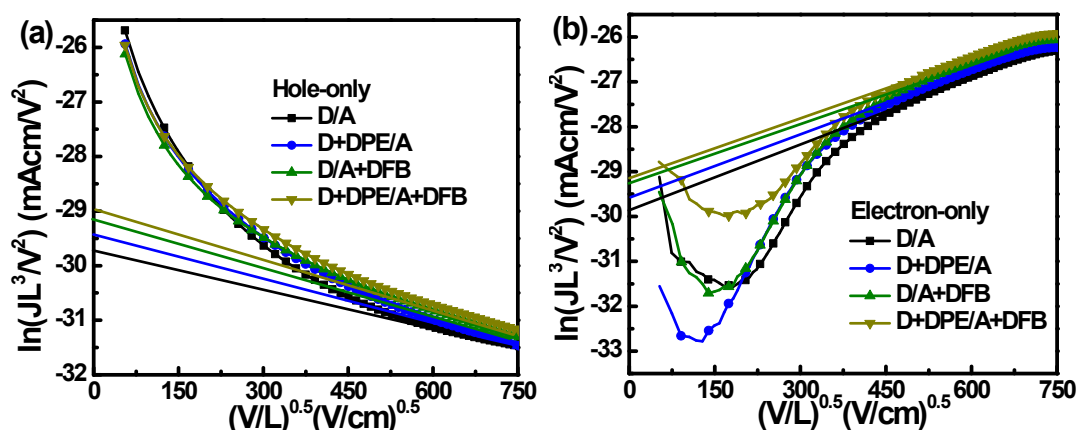


Figure S3. The $\ln(JL^3/V^2)-(V/L)^{0.5}$ curves of (a) hole-only devices and (b) electron-only devices with layered donor and acceptor films

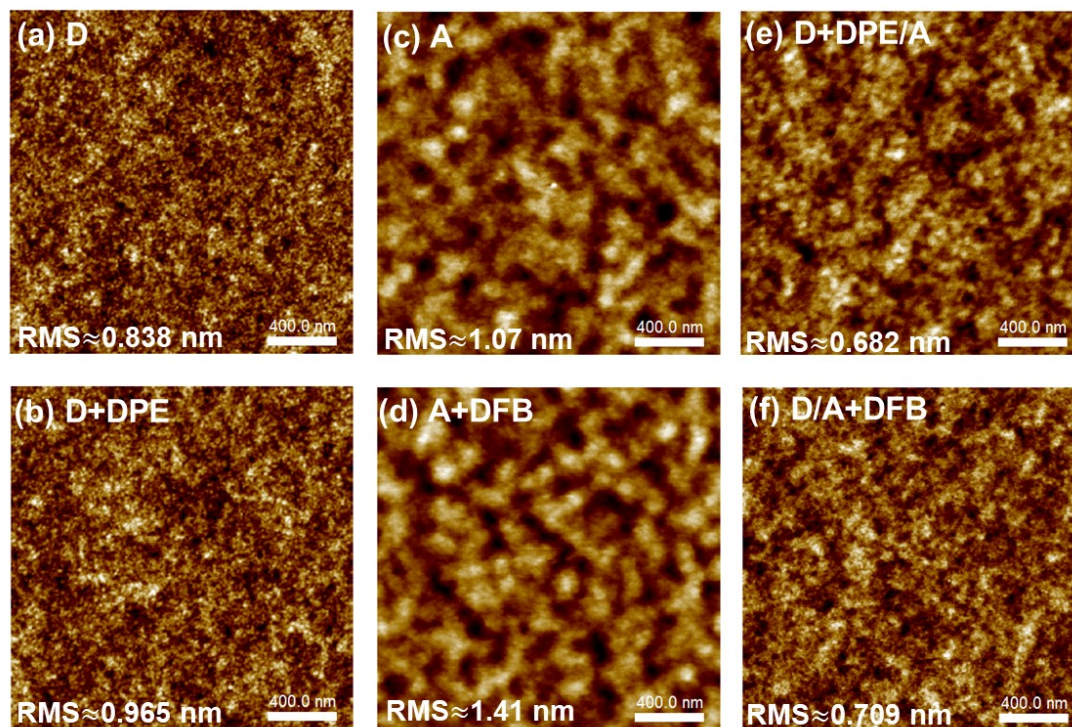


Figure S4. AFM images of (a) D, (b) D+DPE, (c) A, (d)A+DFB (e) D+DPE/A and (f) D/A+DFB

blend films.

Reference:

- [1] Y. Li, H. Huang, M. Wang, W. Nie, W. Huang, G. Fang and D. L. Carroll, *Sol. Energy Mater. Sol. Cells.*, 2012, **98**, 273.
- [2] W. B. Wang, F. J. Zhang, M. D. Du, L. L. Li, M. Zhang, K. Wang, Y. S. Wang, B. Hu, Y. Fang and J. S. Huang, *Nano Lett.*, 2017, **17**, 1995.
- [3] D. W. Sievers, V. Shrotriya and Y. Yang, *J. Appl. Phys.*, 2006, **100**, 114509.
- [4] R. Häusermann, E. Knapp, M. Moos, N. A. Reinke, T. Flatz and B. Ruhstaller, *J. Appl. Phys.*, 2009, **106**, 104507.
- [5] H. Cha, D. S. Chung, S. Y. Bae, M. J. Lee, T. K. An, J. Hwang, K. H. Kim, Y. H. Kim, D. H. Choi and C. E. Park, *Adv. Funct. Mater.*, 2013, **23**, 1556.
- [6] S. Chang, H. Liao, Y. Shao, Y. Sung, S. Hsu, C. Ho, W. Su and Y. Chen, *J. Mater. Chem. A.*, 2013, **1**, 2447.
- [7] Y. Zhang, D. Deng, K. Lu, J. Zhang, B. Xia, Y. Zhao, J. Fang and Z. Wei, *Adv. Mater.*, 2015, **27**, 1071.
- [8] Z. An, J. Yu, S. Jones, S. Barlow, S. Yoo, B. Domercq, P. Prins, L. Siebbeles, B. Kippelen and S. R. Marder, *Adv. Mater.*, 2005, **17**, 2580.
- [9] M. Koppe, H. J. Egelhaaf, G. Dennler, M. C. Scharber, C. J. Brabec, P. Schilinsky and C. N. Hoth, *Adv. Funct. Mater.*, 2010, **20**, 338.
- [10] Y. X. Chen, X. Zhang, C. L. Zhan and J. N. Yao, *ACS Appl. Mater. Interfaces.*, 2015, **7**, 6462.